

192899 mafic granulite, Mount Vernon

(*Youanmi Terrane, Yilgarn Craton*)

Blereau, ER, Korhonen, FJ and Kelsey, DE

Location and sampling

HYDEN (SI 50-4), HURLSTONE (2732)

MGA Zone 50, 711769E 6371083N

Warox Site FJKBGD192899

Sampled on 18 May 2009

This sample was collected from an outcrop on the east side of Mount Vernon, about 52 km northwest of Lake King townsite, 18.4 km southwest of Holt Rock, and 12.3 km east-northeast of Mount Sheridan. The sample was collected as part of the Yilgarn Craton Metamorphic Project (2003–14) undertaken by Ben Goscombe for the Geological Survey of Western Australia (GSWA), and referred to in that study as sample BG09-147c. The results from this project have not been released by GSWA, although select data have been published in Goscombe et al. (2019). This sample is not available in the GSWA collections; all observations are based on descriptions presented in Goscombe et al. (2019) and have not been directly verified.

Geological context

The unit sampled is a mafic granulite of the western Youanmi Terrane (Quentin de Gromard et al., 2021). This unit is part of a belt of Archean metasedimentary and gneissic rocks previously assigned to the South West Terrane and referred to informally by Wilde and Pidgeon (1987) as the ‘Wheat Belt’ region (cf. Wilde, 2001). However, a recent reinterpretation places the boundary between the South West and the Youanmi Terranes farther to the southwest than shown on older maps (Quentin de Gromard et al., 2021). The Youanmi Terrane contains both granite–greenstone and high-grade gneiss components with emplacement ages from 3010 to 2600 Ma (GSWA, 2020; Cassidy et al., 2006). Existing geochronological data from this part of the Youanmi Terrane is sparse. A biotite metagranodiorite, collected about 103 km to the southeast of this locality, yielded an igneous crystallization age of 2978 ± 5 Ma (GSWA 224357, Lu et al., 2018). Two samples of garnet-bearing alkali feldspar granite from Griffins Find approximately 94 km to the west-southwest yielded crystallization ages of c. 2636 Ma (Qiu and McNaughton, 1999). A quartzite also collected from Griffins Find yielded detrital zircon dates between c. 3812 and 2643 Ma, and a conservative maximum age of deposition of 2655 ± 11 Ma (GSWA 198580, Lu et al., 2015b). A pelitic gneiss from Griffins Find yielded detrital zircon dates between c. 2838 and 2629 Ma, and a conservative maximum depositional age of 2638 ± 2 Ma (GSWA 198578; Lu et al., 2015a), and another pelitic gneiss sample yielded a monazite age for high-grade metamorphism of 2641 ± 6 Ma (GSWA 198585, Fielding et al., 2021).

Petrographic description

The sample is a massive medium- to coarse-grained mafic granulite containing pink–grey orthopyroxene, pale green clinopyroxene, plagioclase, green–brown hornblende, with minor orange biotite, quartz and ilmenite (Fig. 1). The sample has a weak grain-shape fabric and a polygonal granoblastic matrix. It is unknown whether the sample has undergone partial melting. Mineral compositions are provided in Table 1.

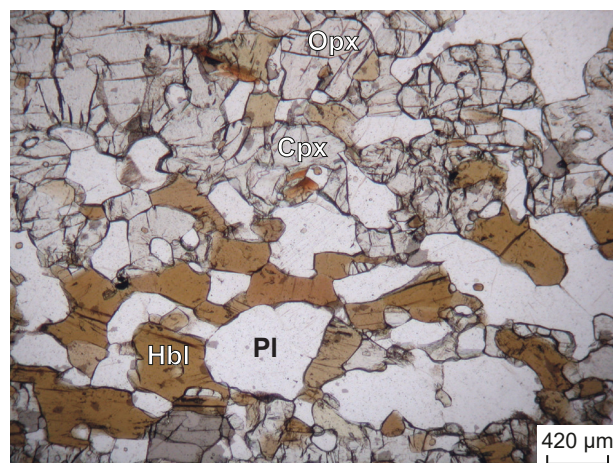


Figure 1. Photomicrograph of sample 192899: mafic granulite, Mount Vernon in plane-polarized light. Mineral abbreviations are explained in the caption to Figure 2

Table 1. Mineral compositions for sample 192899: mafic granulite, Mount Vernon

Mineral ^(a)	Hbl	Hbl	Bt	Bt	Cpx	Cpx	Cpx	Pl	Pl	Ilm	Opx	Opx
Setting	Core	Rim	Core	Rim	Core	Rim	Core	Core	Rim	Matrix	Core	Rim
<i>wt%</i>												
SiO ₂	45.75	47.14	39.87	40.00	52.39	52.54	52.02	54.88	54.32	0.13	52.67	52.54
TiO ₂	2.06	1.93	4.89	4.99	0.24	0.23	0.19	0.00	0.00	52.58	0.16	0.08
Al ₂ O ₃	8.16	7.67	13.18	13.04	1.23	1.11	1.21	28.27	28.50	0.00	0.76	0.63
Cr ₂ O ₃	0.00	0.00	0.00	0.00	0.00	0.00	0.00	0.00	0.00	0.00	0.00	0.00
FeO	9.88	8.69	9.18	9.21	7.31	6.89	7.34	0.09	0.14	40.37	20.58	20.31
MnO	0.10	0.03	0.00	0.02	0.16	0.16	0.15	0.00	0.00	0.84	0.38	0.41
MgO	15.54	15.50	18.22	18.08	15.14	15.24	15.29	0.00	0.00	1.40	24.14	24.06
ZnO	0.01	0.02	0.00	0.00	0.03	0.03	0.02	0.00	0.00	2.85	0.00	0.03
CaO	11.83	11.84	0.00	0.02	22.34	22.60	22.28	11.59	11.89	0.07	0.65	0.56
Na ₂ O	1.29	1.20	0.06	0.01	0.25	0.27	0.26	4.60	4.70	0.09	0.01	0.00
K ₂ O	1.04	1.06	10.05	9.70	0.01	0.00	0.01	0.27	0.24	0.00	0.00	0.02
Total ^(b)	95.67	95.06	95.45	95.07	99.10	99.08	98.77	99.69	99.79	98.32	99.36	98.64
Oxygen	23	23	11	11	6	6	6	8	8	3	6	6
Si	6.70	6.91	2.89	2.90	1.95	1.96	1.94	2.50	2.47	0.00	1.95	1.96
Ti	0.23	0.21	0.27	0.27	0.01	0.01	0.01	0.00	0.00	1.01	0.00	0.00
Al	1.41	1.33	1.12	1.12	0.05	0.05	0.05	1.52	1.52	0.00	0.03	0.03
Cr	0.00	0.00	0.00	0.00	0.00	0.00	0.00	0.00	0.00	0.00	0.00	0.00
Fe ^{3+(c)}	0.54	0.34	0.03	0.03	0.05	0.04	0.07	0.00	0.00	0.00	0.05	0.05
Fe ²⁺	0.67	0.73	0.53	0.53	0.18	0.17	0.16	0.00	0.01	0.86	0.58	0.59
Mn ²⁺	0.01	0.00	0.00	0.00	0.00	0.01	0.00	0.00	0.00	0.02	0.01	0.01
Mg	3.39	3.39	1.97	1.95	0.84	0.85	0.85	0.00	0.00	0.05	1.33	1.34
Zn	0.00	0.00	0.00	0.00	0.00	0.00	0.00	0.00	0.00	0.05	0.00	0.00
Ca	1.86	1.86	0.00	0.00	0.89	0.90	0.89	0.56	0.58	0.00	0.03	0.02
Na	0.37	0.34	0.01	0.00	0.02	0.02	0.02	0.41	0.41	0.00	0.00	0.00
K	0.19	0.20	0.93	0.90	0.00	0.00	0.00	0.02	0.01	0.00	0.00	0.00
Total	15.38	15.31	7.74	7.70	4.00	4.00	4.00	5.00	5.00	2.00	4.00	4.00
<i>Compositional variables</i>												
XFe ^(d)	0.16	0.18	0.21	0.21	0.18	0.17	0.16	–	–	0.94	0.30	0.30

NOTES: – not applicable

(a) Mineral abbreviations explained in the caption to Figure 2

(b) Totals on anhydrous basis

(c) Hornblende cations calculated following Holland and Blundy (1994); Fe³⁺ contents for biotite assumed to be 10% of Fe total;

Fe³⁺ contents for other minerals based on Droop (1987)

(d) XFe = Fe²⁺/(Fe²⁺ + Mg)

Analytical details

Preliminary P – T estimates were obtained using multiple-reaction thermobarometry calculated from the mineral compositions (Table 1; Goscombe et al., 2019). These estimates were derived from the ‘averagePT’ module (avPT) in the program THERMOCALC version tc325 (Powell and Holland, 1988), using the internally consistent Holland and Powell (1998) dataset.

The metamorphic evolution of this sample has been subsequently re-evaluated using phase equilibria modelling, based on the bulk-rock composition (Table 2). The bulk-rock composition was determined by X-ray fluorescence spectroscopy, together with loss on ignition (LOI). The modelled O content (for Fe^{3+}) was set to be 20% of the measured total Fe; the modelled H_2O content was the measured LOI. The bulk composition was adjusted for the presence of apatite by applying a correction to CaO (Table 2). Thermodynamic calculations were performed in the NCKFMASHTO (Na_2O – CaO – K_2O – FeO – MgO – Al_2O_3 – SiO_2 – H_2O – TiO_2 – O) system using THERMOCALC version tc340 (Powell and Holland, 1988; updated October 2013) and the internally consistent thermodynamic dataset of Green et al. (2016; version dataset tc-ds63, created January 2015). The activity–composition relations used in the modelling are detailed in Green et al. (2016), with the augite model used for clinopyroxene. Additional information on the workflow with relevant background and methodology are provided in Korhonen et al. (2020).

Table 2. Measured whole-rock and modelled compositions for sample 192899: mafic granulite, Mount Vernon

<i>XRF whole-rock composition (wt%)^(a)</i>												
SiO₂	TiO₂	Al₂O₃	Fe₂O₃^(b)	FeO^(b)	MnO	MgO	CaO	Na₂O	K₂O	P₂O₅	LOI	Total
49.90	0.65	13.10	–	10.26	0.17	11.80	8.84	1.72	0.34	0.08	0.20	97.06
<i>Normalized composition used for phase equilibria modelling (mol%)</i>												
SiO₂	TiO₂	Al₂O₃	O^(c)	FeO^(d)	MnO	MgO	CaO^(e)	Na₂O	K₂O	–	H₂O^(f)	Total
51.93	0.51	8.03	0.80	8.03	--	18.31	9.74	1.73	0.23	--	0.69	100

NOTES: (a) Data and analytical details are available from the WACHEM database <<http://geochem.dmp.wa.gov.au/geochem/>>
 (b) FeO content is total Fe
 (c) O content (for Fe_2O_3) set to be 20% of measured $\text{FeO}^{(b)}$
 (d) FeO^{T} = moles FeO + 2 * moles O
 (e) CaO modified to remove apatite: $\text{CaO}(\text{Mod}) = \text{CaO}(\text{Total}) - (\text{moles CaO}(\text{in Ap}) = 3.33 * \text{moles P}_2\text{O}_5)$
 (f) H_2O content is the measured LOI
 – not applicable

Results

The P – T pseudosection for sample 192899 was calculated over a P – T range of 2–8 kbar and 650–900 °C (Fig. 2). The solidus is located between 795 and 880 °C across the range of modelled pressures. Rutile is stable above 5.6 kbar at 650 °C and 7 kbar at 870 °C. Garnet is stable in rutile-bearing fields above 7.1 kbar at 650 °C, extending to higher pressures with increasing temperature. Biotite is consumed at temperatures above the solidus, followed by quartz with increasing temperature.

Metamorphic P – T estimates ($\pm 2\sigma$ uncertainty) calculated using multiple-reaction thermobarometry are 5.3 ± 1.1 kbar and 749 ± 17 °C (Goscombe et al., 2019). These calculations used matrix rim compositions (Table 1) to estimate peak conditions. Core compositions yield a slightly lower pressure estimate (3.2 ± 2.0 kbar, 762 ± 41 °C; Goscombe et al., 2015), tentatively interpreted to record prograde conditions.

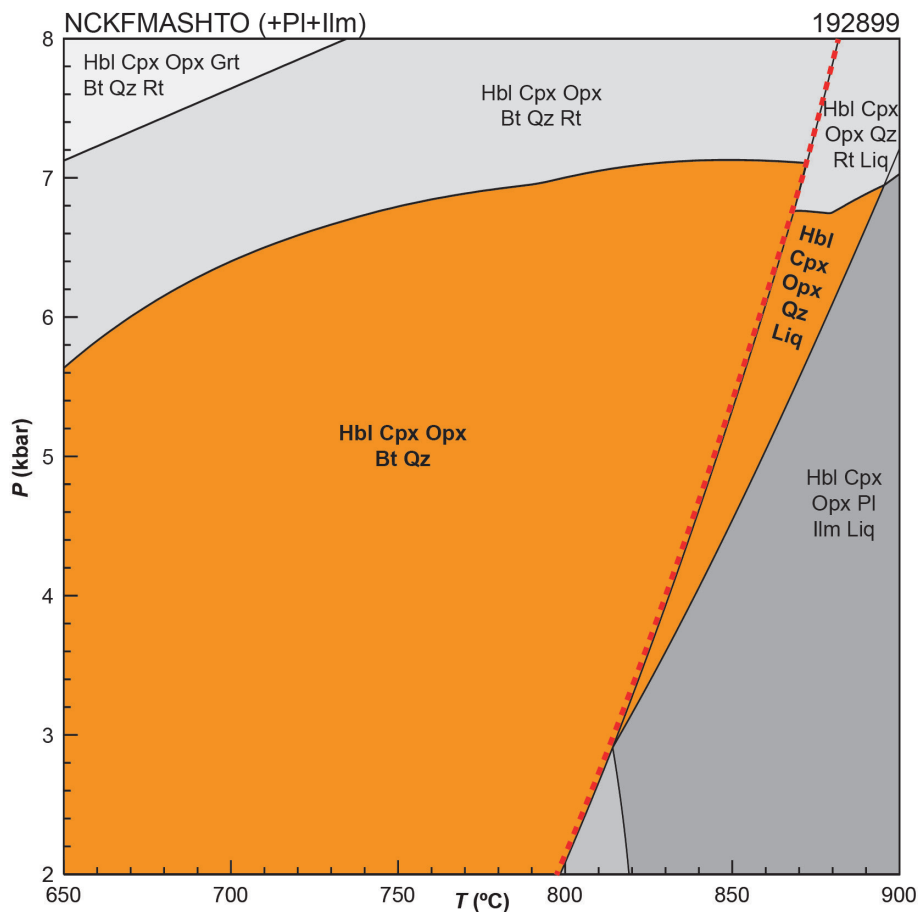


Figure 2. *P*–*T* pseudosection calculated for sample 192899: mafic granulite, Mount Vernon. Assemblage fields corresponding to peak metamorphic conditions are delimited by bold text and orange shading. Red dashed line represents the solidus. Abbreviations: Bt, biotite; Cpx, clinopyroxene; Grt, garnet; Hbl, hornblende; Ilm, ilmenite; Liq, silicate melt; Opx, orthopyroxene; Pl, plagioclase; Qz, quartz; Rt, rutile

Interpretation

The peak metamorphic assemblage is interpreted to be hornblende–clinopyroxene–orthopyroxene–plagioclase–ilmenite–quartz(–biotite–melt). There is uncertainty whether the sample has undergone partial melting. There is also no available information on the petrographic setting of biotite or its relationship with the other minerals. The subsolidus hornblende–clinopyroxene–orthopyroxene–plagioclase–ilmenite–biotite–quartz field is stable up to 870 °C below 7.1 kbar, and the hornblende–clinopyroxene–orthopyroxene–plagioclase–ilmenite–quartz–melt field is stable between 815 and 895 °C at 2.9 – 7.0 kbar (Fig. 2). Both fields are delimited by the stability of rutile at higher pressure, and the upper temperature limit is constrained by the loss of quartz.

The metamorphic *P*–*T* estimates calculated using multiple-reaction thermobarometry fall within the inferred peak subsolidus assemblage of hornblende–clinopyroxene–orthopyroxene–plagioclase–ilmenite–biotite–quartz. There is no information on the prograde and retrograde segments of the *P*–*T* path, and therefore the overall shape of the *P*–*T* path is not defined. The *P*–*T* results retrieved from the compositions of mineral cores and rims may broadly suggest an anticlockwise path, although these results are within uncertainty.

Based on the results of phase equilibria modelling, peak metamorphic conditions are poorly constrained, with estimates below 870 °C and 7.1 kbar, defining a minimum apparent thermal of 120 °C/kbar. Mineral compositions are consistent with equilibration at 749 ± 17 °C, 5.3 ± 1.1 kbar, defining an apparent thermal between 110 and 170 °C/kbar; these constraints are considered to be the best results available, although it is possible that they do not record peak conditions.

References

- Cassidy, KF, Champion, DC, Krapež, B, Barley, ME, Brown, SJA, Blewett, RS, Groenewald, PB and Tyler, IM 2006, A revised geological framework for the Yilgarn Craton, Western Australia: Geological Survey of Western Australia, Record 2006/8, 8p.
- Droop, GTR 1987, A general equation for estimating Fe³⁺ concentrations in ferromagnesian silicates and oxides from microprobe analyses, using stoichiometric criteria: Mineralogical Magazine, v. 51, no. 361, p. 431–435.
- Fielding, IOH, Wingate, MTD, Korhonen, FJ and Rankenburg, K 2021, 198585: pelitic gneiss, Griffins Find; Geochronology Record 1767: Geological Survey of Western Australia, 5p.
- Geological Survey of Western Australia 2020, Youanmi, 2020: Geological Survey of Western Australia, Geological Information Series, digital data package.
- Goscombe, B, Blewett, R, Groenewald, PB, Foster, D, Wade, B, Wyche, S, Wingate, MTD and Kirkland, CL 2015, Metamorphic Evolution of the Yilgarn Craton: Geological Survey of Western Australia, 910p. (unpublished).
- Goscombe, B, Foster, DA, Blewett, R, Czarnota, K, Wade, B, Groenewald, B and Gray, D 2019, Neoarchean metamorphic evolution of the Yilgarn Craton: a record of subduction, accretion, extension and lithospheric delamination: Precambrian Research, article no. 105441, doi:10.1016/j.precamres.2019.105441.
- Green, ECR, White, RW, Diener, JFA, Powell, R, Holland, TJB and Palin, RM 2016, Activity-composition relations for the calculation of partial melting equilibria in metabasic rocks: Journal of Metamorphic Geology, v. 34, no. 9, p. 845–869.
- Holland, T and Blundy, J 1994, Non-ideal interactions in calcic amphiboles and their bearing on amphibole-plagioclase thermometry: Contributions to Mineralogy and Petrology, v. 116, no. 4, p. 433–447.
- Holland, TJB and Powell, R 1998, An internally consistent thermodynamic data set for phases of petrological interest: Journal of Metamorphic Geology, v. 16, no. 3, p. 309–343.
- Korhonen, FJ, Kelsey, DE, Fielding, IOH and Romano, SS 2020, The utility of the metamorphic rock record: constraining the pressure–temperature–time conditions of metamorphism: Geological Survey of Western Australia, Record 2020/14, 24p.
- Lu, Y, Wingate, MTD, Kirkland, CL, Goscombe, B and Wyche, S 2015a, 198578: pelitic gneiss, Griffins Find; Geochronology Record 1284: Geological Survey of Western Australia, 4p.
- Lu, Y, Wingate, MTD, Kirkland, CL, Goscombe, B and Wyche, S 2015b, 198580: quartzite, Griffins Find; Geochronology Record 1285: Geological Survey of Western Australia, 5p.
- Lu, Y, Wingate, MTD and Smithies, RH 2018, 224357: biotite metagranodiorite, Phillips River; Geochronology Record 1550: Geological Survey of Western Australia, 4p.
- Powell, R and Holland, TJB 1988, An internally consistent dataset with uncertainties and correlations: 3. Applications to geobarometry, worked examples and a computer program: Journal of Metamorphic Geology, v. 6, no. 2, p. 173–204.
- Quentin de Gromard, R, Ivanic, TJ and Zibra, I 2021, Interpreted bedrock geology of the southwest Yilgarn Craton: Geological Survey of Western Australia, in press.
- Qiu, Y and McNaughton, NJ 1999, Source of Pb in orogenic lode-gold mineralisation: Pb isotope constraints from deep crustal rocks from the southwestern Archaean Yilgarn Craton, Australia: Mineralium Deposita, v. 34, p. 366–381.
- Wilde, SA 2001, Jimpending and Chittering metamorphic belts, Western Australia - a field guide: Geological Survey of Western Australia, Record 2001/12, 24p.
- Wilde, SA and Pidgeon, RT 1987, U–Pb geochronology, geothermometry and petrology of the main areas of gold mineralization in the ‘Wheat Belt’ region of Western Australia: Western Australian Minerals and Petroleum Research Institute; Project 30, Final Report, 171p.

Links

Metamorphic history introduction document: [Intro_2020.pdf](#)

Recommended reference for this publication

Blereau, ER, Korhonen, FJ and Kelsey DE 2021, 192899: mafic granulite, Mount Vernon; Metamorphic History Record 5: Geological Survey of Western Australia, 6p.

Data obtained: 19 May 2020

Date released: 25 June 2021

This Metamorphic History Record was last modified on 9 June 2021.

Grid references in this publication refer to the Geocentric Datum of Australia 1994 (GDA94). All locations are quoted to at least the nearest 100 m.

WAROX is GSWA's field observation and sample database. WAROX site IDs have the format 'ABCXXXnnnnnnSS', where ABC = geologist username, XXX = project or map code, nnnnnn = 6 digit site number, and SS = optional alphabetic suffix (maximum 2 characters).

Isotope and element analyses are routinely conducted using the GeoHistory laser ablation ICP-MS and Sensitive High-Resolution Ion Microprobe (SHRIMP) ion microprobe facilities at the John de Laeter Centre (JdLC), Curtin University, with the financial support of the Australian Research Council and AuScope National Collaborative Research Infrastructure Strategy (NCRIS). The TESCAN Integrated Mineral Analyser (TIMA) instrument was funded by a grant from the Australian Research Council (LE140100150) and is operated by the JdLC with the support of the Geological Survey of Western Australia, The University of Western Australia (UWA) and Murdoch University. Mineral analyses are routinely obtained using the electron probe microanalyser (EPMA) facilities at the Centre for Microscopy, Characterisation and Analysis at UWA, and at Adelaide Microscopy, University of Adelaide.

Digital data related to WA Geology Online, including geochronology and digital geology, are available online at the Department's [Data and Software Centre](#) and may be viewed in map context at [GeoVIEW.WA](#).

Disclaimer

This product uses information from various sources. The Department of Mines, Industry Regulation and Safety (DMIRS) and the State cannot guarantee the accuracy, currency or completeness of the information. Neither the department nor the State of Western Australia nor any employee or agent of the department shall be responsible or liable for any loss, damage or injury arising from the use of or reliance on any information, data or advice (including incomplete, out of date, incorrect, inaccurate or misleading information, data or advice) expressed or implied in, or coming from, this publication or incorporated into it by reference, by any person whatsoever.



© State of Western Australia (Department of Mines, Industry Regulation and Safety) 2021

With the exception of the Western Australian Coat of Arms and other logos, and where otherwise noted, these data are provided under a Creative Commons Attribution 4.0 International Licence. (<http://creativecommons.org/licenses/by/4.0/legalcode>)

Further details of geoscience products are available from:

Information Centre
Department of Mines, Industry Regulation and Safety
100 Plain Street
EAST PERTH WA 6004
Telephone: +61 8 9222 3459 | Email: publications@dmirs.wa.gov.au
www.dmirs.wa.gov.au/GSWApublications